

1 **Title:** Ubitrail: A robust and open-source software for tracking insect locomotion

2

3 **Authors:** Joe D. Gallagher<sup>\*1</sup>, Michael T. Siva-Jothy<sup>1</sup>, and Quentin Geissmann<sup>2</sup>

4

5 **Author affiliations:**

6 <sup>1</sup> *Department of Animal and Plant Sciences, University of Sheffield, S10 2TN, U.K.*

7 <sup>2</sup> *Department of Life Sciences, Imperial College, South Kensington, London, SW7 2AZ, U.K.*

8

9 <sup>\*</sup>Corresponding author: joedgallagher@gmail.com

10

## 11 **Abstract**

12 Analysing the locomotor behavior of animals is essential to a diverse range of studies, from learning  
13 and memory to reproduction and immunity. Automated tracking systems can provide a high-  
14 throughput method of obtaining quantitative behavioural data, but many of the currently available  
15 options are inflexible, difficult to use, or expensive. We present an open-source software ('Ubitrail')  
16 for tracking the individual movement of insects, and a statistical package ('Rubitrail') for extracting  
17 and analysing behavioural metrics of interest. The software is designed to be versatile with regards  
18 to species morphology and experimental design and robust to imperfect conditions of video capture,  
19 as well as inexpensive and straightforward to use. We provide a demonstration of its capabilities by  
20 using it to detect an effect of immune challenge upon locomotion in the mealworm beetle, *Tenebrio*  
21 *molitor*. Finally, we investigate the biological significance of relationships between our extracted  
22 behavioural metrics by comparing endogenous beetle locomotion to computer-generated  
23 simulations of locomotion.

24

25 **Keywords:** locomotory analysis; video tracking; *Tenebrio molitor*; sickness behaviours

## 26 1. Introduction

27 Locomotor activity impacts almost all aspects of a mobile animal's ecology. Movement underpins  
28 key fitness-driving traits, such as foraging, mating, courtship, learning processes, and immunity  
29 (Martin, 2004). Many of the most commonly measured behaviours in animals, such as ambulation,  
30 freezing (resting immobile), jumping, vectorial information (speed, acceleration), positional  
31 information (e.g. site preference, orientation angle) – as well as psychological measures typically  
32 considered in only vertebrate studies, such as anxiety, obsession and aggression – are emergent  
33 from tracking the movement vectors of an individual, i.e. the organism's spatial coordinates over  
34 time.

35 The quantification of the complex movement patterns of mobile organisms has become an  
36 integral subject in biological research, and has been facilitated by recent advances in automated  
37 tracking methods. Automated systems provide a much higher throughput than manual methods, and  
38 tend to be more reliable due to the consistency of a processing algorithm, which does not suffer  
39 observer fatigue or drift (Noldus *et al.*, 2001). Digital methods can also yield behavioural metrics  
40 that would be difficult or impossible to quantify manually, such as velocity, acceleration and turning  
41 angle, as well as calculating time and spatial location with a high degree of accuracy.

42 As computing capabilities have increased and costs decreased over the last decade,  
43 automated tracking systems have progressed from rudimentary and often unreliable analogue  
44 systems which described mostly discrete behaviours, to digitised methods which can detail an array  
45 of continuous kinematic variables. Advancements in computer-vision capabilities and the increasing  
46 availability and support of open-source libraries, such as OpenCV (Willowgarage,  
47 <http://opencv.willowgarage.com>), are creating a new and accessible ecosystem of highly  
48 customisable and affordable tools for biologists to study the behaviour of a much larger variety of  
49 organisms. Several digitiser-based video tracking systems are commercially available, but there are  
50 drawbacks with many of these.

51 Firstly, many trackers are developed only for the most well-studied model organisms (e.g.  
52 *Drosophila* [Gomez-Marin *et al.*, 2012, Dankert *et al.*, 2009], *C. elegans* [Swierczek, *et al.*, 2011],  
53 zebrafish [Beyan & Fisher, 2013], mice [de Chaumont *et al.*, 2012]), being highly tailored to the  
54 particular morphology and movement patterns of their target species. Secondly, many of these  
55 programs are designed to address specific behavioural paradigms, and thus offer little flexibility,  
56 often requiring specialised apparatus or the use of highly specific experimental designs. Thirdly,  
57 much available tracking software is proprietary and requires a substantial up-front fee, as well as  
58 continuing license fees in some cases (e.g. EthoVision [Noldus *et al.*, 2001], ANY-maze  
59 [<http://anymaze.com>], GroupScan, LoliTrack, PhenoTracker). Of the open-source options available,  
60 several use proprietary toolboxes to parse output files (containing the tracked X,Y-coordinates),  
61 most notably MATLAB (e.g. Ctrax [Branson *et al.*, 2012], CADABRA, idTracker, Motr, SOS-  
62 track). Finally, several open-source software are largely inflexible and onerous to modify,  
63 necessitating in-depth knowledge of the relevant programming language as well as a substantial  
64 investment of time (e.g. Flydra), or are currently unstable or non-functional due to a lack of  
65 maintenance (e.g. SwisTrack [Lochmatter *et al.*, 2008], MotMot [Straw & Dickinson, 2009]).

66 In this paper, we describe an open-source software, 'Ubitrail', for the automated tracking of  
67 insect locomotion and a statistical package, 'Rubitrail', for extracting behavioural metrics. The  
68 platform is intended to be: (i) versatile, working with a range of morphologically and ethologically  
69 distinct insect species and within a range of non-specialised experimental set-ups; (ii) robust,  
70 working under imperfect lighting conditions and handling insect occlusion and other experimental  
71 imperfections which can lower accuracy; (iii) simple, with a simple graphical user interface offered  
72 for tracking and statistical functions allowing for straightforward analysis straight 'out of the box';  
73 and (iv) affordable, making use of exclusively open-source software and relying on inexpensive  
74 hardware. We provide a proof of concept by quantifying changes in locomotion following immune  
75 challenge in the mealworm beetle, *Tenebrio molitor*, in order to investigate sickness behaviours. By

76 comparing this data with computer-generated simulations of locomotion, we help separate  
77 meaningful biological relationships between behavioural metrics from mathematical correlations in  
78 order to validate the behavioural metrics defined.

79

80

## 81 **2. Methods**

82

### 83 **2.1. Description of the system**

84 The tracking software, UbiTrail, was written in C++ using the OpenCV library (Willowgarage,  
85 <http://opencv.willowgarage.com>), and under the CodeBlocks design environment  
86 (<http://codeblocks.org>). The software source code and compilers for Unix and Microsoft Windows  
87 operating systems are freely available online (<http://sourceforge.net/projects/ubitrail>), as is the  
88 associated R package, Rubitrail, as well as a user manual, sample videos and sample data.

89 The details of the image analysis process are described in detail in Figure 1. In brief, the  
90 software uses a dynamic learning algorithm to learn to identify moving foreground objects during  
91 an initial training period (default value of 500 frames, ~25 seconds). In order to solve ambiguities in  
92 foreground detection, a likelihood model is built on the fly, based upon several key features of  
93 known foreground, including contour shape, pixel colour and distance between current contour and  
94 last detected contour, with the most likely single contour being identified as foreground.

95

### 96 **2.2. Using the software**

97 UbiTrail currently works with digital video files as input, which can be recorded using an  
98 inexpensive USB video camera (any webcam with a resolution of at least 640x480 pixels is  
99 suitable) and are easily captured using the open-source multimedia player, VLC (VideoLAN,  
100 <http://videolan.org/vlc>).

101           After recording a video, the user is able to define a mask to denote the position of areas  
102 within the arena, as well as sub-territories within individual areas, if desired. The user is then able to  
103 adjust several processing parameters in order to optimise tracking accuracy, such as sensitivity  
104 (which determines how likely noise is to be detected as motion) and the number of frames used to  
105 train the motion detector.

106           The software can be implemented either via the command line or using a graphical user  
107 interface (GUI). The GUI is a simple assistant which allows the user to interactively define the  
108 inputs and output options, preview the defined mask over the video, and visualise the actual  
109 tracking process on-the-fly (Figure 2). Command line usage can increase efficiency by allowing the  
110 user to iteratively analyse multiple videos without the need for continual input.

111           The software outputs a CSV file containing an X,Y coordinate, timestamp, area ID and  
112 territory ID (if applicable) for each detected object in each frame of a video. Also included is a  
113 header containing metainformation, such as name, duration, and number of frames per second, as  
114 well as the X,Y-coordinates of each detected area. Video files of the tracking process can also be  
115 optionally returned, either as a single video of the global arena or as separate videos for each  
116 individual area.

117

### 118 **2.3. Rubitrail analysis package**

119 The analysis software, Rubitrail, is a package written for R (R Core Development Team, [http://r-](http://r-project.org)  
120 [project.org](http://r-project.org)). The package extracts multiple features from the raw data outputted by the tracking  
121 software, including velocity, turning angles, activity levels and positional information, as well as  
122 allowing the user to define their own additional variables for analysis. Whilst all scripts within the  
123 package are fully customisable, a single master function is included to aid user accessibility,  
124 requiring as input only a list of CSV files for analysis and a scale calibration (pixels/mm).

125

### 126 2.3.1. *Pre-processing data*

#### 127 2.3.1.1. *Undistortion*

128 Fisheye lenses and low-cost wide-angle lenses can produce a significant degree of barrel distortion  
129 in the images they capture, having the potential to impact the validity of detected movements in a  
130 tracking software (Figure 3). This can be corrected using a simple algorithmic transformation:



131 where  $r$  is the distance of a given pixel to the centre of the uncorrected image and  $R$  is the distance  
132 of the pixel in the corrected image. This transformation can either be applied before tracking  
133 analysis by transforming each image frame of the raw video, or after tracking by transforming the  
134 detected X,Y-coordinates; Rubitrail utilises the latter method. Ready-made parameter sets for  
135 particular cameras can be found online (e.g. [http://sourceforge.net/projects/hugin/files/PTLens](http://sourceforge.net/projects/hugin/files/PTLens%20Database)  
136 [%20Database](http://sourceforge.net/projects/hugin/files/PTLens%20Database)), or can be calculated manually by taking a calibration image (see Figure 3) and  
137 identifying the most suitable values using the undistortion feature available in a number of image  
138 manipulation programs (e.g. ImageMagic [<http://imagemagick.org>]).

139

#### 140 2.3.1.2. *Linear interpolation*

141 In frames where insects are occluded by obstacles or glare, or a contour is otherwise not found, X,Y  
142 position is inferred using linear interpolation. X,Y-coordinates are not inferred for training frames,  
143 where the insect has yet to be detected. In instances where no movement is detected throughout the  
144 entire video, a velocity of zero is inferred for all frames whilst all other metrics regarding positional  
145 information are defined as NA. In cases where movement is not detected in the final frames of a  
146 video (e.g. the insect does not move in the final two minutes of analysis), the X,Y-coordinates for  
147 the remaining frames are inferred as the last confirmed location of the insect.

148

### 149 2.3.1.3. Trajectory smoothing

150 Camera noise, lighting abnormalities, non-locomotory insect movements (e.g. grooming,  
151 antennation), and imperfections in foreground segmentation can cause false movements to be  
152 identified, increasing the noise in detected X,Y trajectories. Furthermore, lateral oscillation in the  
153 detection of moving objects is common, which may be due to alternated movement between the  
154 posterior and anterior of an insect between frames (Hen *et al.*, 2004). Both of these factors are  
155 manifest in the tracked coordinates as a relatively small jitter, with perturbations no larger than the  
156 maximum length of the tracked insect. Two steps were taken to correct for this noise.

157 Firstly, trajectories were smoothed by using a simple moving median (e.g. Hen *et al.*, 2004)  
158 with a window size of 20 data points (1 s) a 1 point step size (0.05 s), which allowed maximum  
159 overlap between smoothing windows. These values were found to preserves overall trajectory  
160 information and provide greater accuracy in determining velocity, turning angles and overall  
161 activity level (Figure 4). Secondly, due to the size of the smoothing window, insects were often  
162 falsely determined to have negligible, but non-zero, velocity ( $> 0$  mm/s). A movement threshold  
163 was thus implemented to filter such negligible movements from the smoothed velocity data, with  
164 near-zero velocities of  $< 1$  mm/s ( $\sim 2$  pixels/s; a value used in similar tracking software [Valente *et*  
165 *al.*, 2007; Robie *et al.*, 2010; Colomb *et al.*, 2012]) being redefined as zero velocity ( $=0$ mm/s)  
166 (Figure 5).

167

### 168 2.3.2. Extracting metrics

169 Several key metrics to describe insect locomotion were defined and extracted from the smoothed  
170 trajectory data.

171

#### 172 2.3.2.1. Velocity metrics

173 Distance moved was calculated as the Pythagorean distance between smoothed X,Y-coordinates in

174 successive frames. Summing each movement length over the entire analysis yielded the total  
175 distance travelled (mm). Dividing distance travelled per frame by time elapsed gave instant velocity  
176 (mm/s), and the first derivative of instant velocity was used to define acceleration (mm/s<sup>2</sup>).  
177

#### 178 2.3.2.2. Angular metrics

179 Turning angle was calculated as the angle between successive velocity vectors (Figure 6).  
180 Considering the movement from P<sub>0</sub> to P<sub>1</sub>,  $\alpha_0$  is the absolute movement angle, the turning angle,  $\gamma$ ,  
181 can be calculated as  $\alpha_0 - \alpha_1$ . Movement paths of walking insects are generally continuous, and do  
182 not have discrete break points that make it easy to define moves; a common solution is to resample  
183 movement at regular time intervals and connect successive positions with linear interpolation.  
184 Turning angles were therefore calculated from smoothed data which was down-sampled to a rate of  
185 1 frame per second (Figure 6). Meander is a measure of movement tortuosity which combines  
186 turning angle with distance travelled, and increased meander has been associated with navigational  
187 uncertainty (Collins *et al.*, 1994). Meander was calculated by dividing the turning angle by the  
188 instantaneous velocity ( $\theta$  \* mm/s) (Martin *et al.*, 2004). Many animals show a tendency to turn  
189 around an arena (Yaski *et al.*, 2011), a behaviour which is often interpreted as an escape response.  
190 Escape responses are well-studied in cockroaches, which rapidly turn directly away (180°) from  
191 threatening stimuli, such as a puff of wind, and accelerate away (Domenici *et al.*, 2008). A similar  
192 response is observed in *Tenebrio molitor* (pers. obs.), although this behaviour may equally be  
193 representative of roving behaviour or foraging activity, as opposed to an anti-predation or stress  
194 response. Turnaround events were defined as turns of  $180^\circ \pm 25^\circ$  which were completed within the  
195 space of one second (example highlighted in Figure 6e).  
196

#### 197 2.3.2.3. Activity metrics

198 Run length encoding (RLE) was used to temporally smooth velocity in order to derive activity



metrics, allowing identification of stationary and mobile phases. RLE is a form of data compression which identifies patterns in consecutive sequences (runs) of data. For example, a binary sequence of characters, <AAAAABBABBB>, may be run length encoded as, <5A, 2B, 1A, 3B>. Here, information on mobility was calculated by run length encoding smoothed and thresholded velocity data to determine whether movement speeds were above or below a user-defined velocity threshold (1 mm/s) (Figure 7). Owing to noise between frames in detected velocities, a sliding window of 3 s was used to classify movement transitions (see Figure 8); i.e. when velocity was above the defined threshold ( $\geq 1$  mm/s) threshold for a period of  $\geq 3$  s, the insect entered a movement phase, and when its speed fell below 1mm/s for a period of  $\geq 3$  s, the insect entered a stationary phase. The absolute number of phases transitions and mean duration of mobile and stationary phases was calculated for each insect.

210

#### 211 2.3.2.4. *Spatial analysis*

'Heat maps' can be outputted to provide a fast and intuitive overview of an insect's location during the course of the experiment (Figure 9). Two metrics, thigmotaxis and exploration, were also developed in order to quantify the amount of time spent in certain zones of the arena. Thigmotaxis is the tendency of many animals to remain in the perimeter of an arena during open-field experiments, moving in the peripheral areas where they can maintain physical contact with the walls of the arena and avoiding central zones whose open space may leave the insect more vulnerable to predation (e.g. Gotz & Biesinger, 1985; Colomb *et al.*, 2012). Exploratory (or roving) behaviour is often defined in vertebrates alongside such metrics as shyness/boldness, aggression and neophobia (Dingemanse *et al.*, 2002), but may be more simply defined as the proportion of the environment traversed.

In order to normalise the spatial locations for each arena, a minimum enclosing circle was fitted to each arena to determine its exact boundaries, before tracked Cartesian coordinates (x,y) for

each arena were converted to polar coordinates ( $r, \theta$ ). To quantify thigmotaxis, each defined minimum enclosing circle was divided into two zones of equal area: an inner disc and an outer ring (Figure 10), and each  $r, \theta$ -coordinate was defined as belonging in the inner or outer zone based upon its distance from the centre of the arena. The thigmotaxis metric ranges from 0 to 1, where 1 represents the insect remaining at the perimeter of the arena for the entire observation period and 0 remaining only in the arena centre.

To quantify exploration, each circular arena was divided into a network of 96 cells of equal area by a series of concentric circles and line segments (Figure 11). The grid cell location of each  $r, \theta$ -coordinate in a trajectory path is determined, and a measurement of proportion of territory visited (number of unique cells visited / total number of cells) is calculated for each insect over the course of observation.

## **2.4. Validating the software**

### ***2.4.1. Testing tracking accuracy***

Implemented smoothing and thresholding procedures acted to eliminate the majority of false artifacts from raw trajectories. To quantify the remaining level of unreliability in the system and measure its accuracy, the tracker was compared to human users. Videos were manually authenticated by producing a series of images at random points during the analysis, and asking human users to estimate the  $x, y$  position of objects in the image using a simple interactive C++ application (Figure 13). For the same frames, human-estimated object coordinates were compared with raw object coordinates detected by the software, and with processed object coordinates returned after movement thresholding and smoothing in order to gain a correlative measure of accuracy (Figures 14 & 15).

### ***2.4.2. Comparing endogenous locomotion with computer-generated trajectories***

249 An effective way to investigate meaningful relationships between the different behavioural metrics  
250 defined above is to compare endogenous beetle locomotion with computer-generated data (in which  
251 the simulated trajectories represent 'perfect' information consisting of known coordinates), helping  
252 to separate biological relationships in the data from simple mathematical correlations. Computer-  
253 generated trajectories were made using a correlated walk rule by modifying code from the  
254 adehabitatLT package (Calenge et al., 2009) and scripts made available by Colomb et al. (2012).  
255 Walks were fitted by adjusting values for median velocity, median turning angle and median activity  
256 duration until they closely resembled endogenous locomotion. (A sample trajectory is shown in  
257 Figure 16.)

258 Colomb et al. (2012) used two methods of trajectory simulation to compare with the  
259 endogenous locomotion of adult *Drosophila melanogaster*: correlated walks and Levy walks.  
260 Whilst these two methods differ only in terms of their velocity sampling, they can produce  
261 emergent differences in defined behavioural metrics, such as total distance travelled and duration of  
262 activity bouts (Colomb et al., 2012). Here, by using a run length encoded binary sequence to model  
263 the probability of activity (as opposed to a randomly oscillating binary sequence), we are able to  
264 simulate more sustained bursts of movement /non-movement lasting for minutes at a time, which  
265 more closely resembles true beetle locomotion.

266 In order to simulate our experimental data, computer-generated trajectories were bounded  
267 within a circular arena. Starting from an initial starting point at the centre of the arena, the first  
268 turning angle is chosen randomly, with each proceeding angle sampled from a wrapped normal  
269 distribution around the previous angle. The correlation strength between two consecutive turning  
270 angles is determined by a concentration parameter, 'rho', between 0 and 1. The distance moved  
271 between each generated frame is then determined by sampling from a gamma distribution fitted to  
272 endogenous beetle speed data. When a generated x,y-coordinate lies outside the arena limits (i.e.  
273 when  $R_t > r$ , where  $R$  is  $\sqrt{x_t^2 + y_t^2}$  and  $r$  is the radius of the bounded arena), it is replaced by the

274 nearest point within the bounded limits and the next turning angle is resampled randomly.

275         In order to simulate bouts of movement and inactivity, each speed value was multiplied by a  
276 value taken from a run length encoded binary sequence, which was produced in two steps. Firstly,  
277 bout durations of activity and inactivity were generated by sampling from two separate gamma  
278 distributions which model endogenous beetle activity/inactivity durations (two different  
279 distributions were used as bouts of inactivity were generally found to last longer than bouts of  
280 activity in *T. molitor*). Secondly, generated bout durations were alternately sampled to create an  
281 alternating sequence of inactivity frames (zeros) and activity frames (ones). For example, the  
282 inactivity sample <2,3,1> and activity sample <5,2,2> produce the binary sequence  
283 <001111100011011>.

284         The shape ( $\alpha$ ) and rate ( $\beta$ ) parameters of the gamma distributions used to simulate speed and  
285 activity/inactivity duration were optimised by modelling endogenous data with the `fitdistr()`  
286 function of the MASS package (Venables & Ripley, 2002). Thirty trajectory simulations were  
287 generated to compare with endogenous beetle locomotion, with each lasting 10 minutes at 20  
288 frames per second. In order to approach observed endogenous variation in speed and  
289 activity/inactivity duration, the shape and rate values of gamma distributions was set to vary for  
290 each simulated trajectory. The parameters chosen for the simulations were as follows: velocity:  $\alpha =$   
291  $0.695 \pm 0.144$ ,  $\beta = 0.119 \pm 0.0335$  (mean  $\pm$  S.D.); stationary phase duration:  $\alpha = 0.221$ ,  $\beta = 0.00764$ ;  
292 mobile phase duration:  $\alpha = 0.773$ ,  $\beta = 0.0557$ ; angle correlation ( $\rho$ ) = 0.994.

## 293 2.5. Computational efficiency?

### 294 Benchmarking...

295

## 296 2.6. Experimental validation

### 297 2.6.1. *Experimental methods*

298 .....

299

### 300 2.6.2. *Statistical analysis*

301 All statistical analyses were conducted using R v3.1.2 under Ubuntu (R Development Core Team,  
302 2014). Behavioural metrics are described for each individual as either single values (e.g.  
303 thigmotaxis, exploration, number of pauses) or medians of multiple values (e.g. speed, turning  
304 angle, pause duration). Medians were used instead of means to describe these continuous metrics as  
305 they were clearly non-normally distributed.

306 A principal component analysis (PCA) of endogenous locomotion revealed no clear  
307 correlations between behavioural metrics (Figure 18), so the effects of immune challenge and beetle  
308 gender were investigated separately for each behavioural variable. A linear mixed effects was built  
309 for each metric using the lme4 package (Bates et al., 2014), with beetle sex and treatment (and their  
310 interaction) defined as fixed effects and beetle identity defined as a random effect. P-values were  
311 corrected for multiple comparisons in order to control for false discovery (e.g. Benjamini &  
312 Hochberg, 1995).

### 313 3. Results

314

#### 315 3.1. Validation of the tracking software

##### 316 3.1.1. Automated vs. human tracking

317 Comparison between insect identification by the software and by human users..... (Figures 14  
318 & 15).

319

##### 320 3.1. Endogenous vs. simulated locomotion

321 Brief discussion of correlation plots..... (Figures 17). Simulated trajectories help determine  
322 the chance levels of certain complex emergent properties of locomotion, such as thigmotaxis  
323 and exploration, and the how they can be affected by differences in simple locomotion rules,  
324 such as movement speed or pause duration.

325

#### 326 3.2. Sexual dimorphism in *T. molitor* sickness behaviours

327 ... (Figure 19).

328

329

### 330 4. Discussion

331

332 The developed tracker, Ubitrail, is capable of recording the trajectory of up to 24 insects  
333 simultaneously with relatively high spatial (up to 0.5mm / pixel) and temporal resolution (up to  
334 30Hz). A range of biologically meaningful behavioural metrics have been defined in order to  
335 produce quantitative data on insect locomotion, including information on velocity, turning angles  
336 and location, as well as several more specific behaviours such as turnarounds, thigmotaxis and  
337 exploration.

338

339 The tracker is: (i) versatile, having been tested on a range of insect species, including *Tenebrio*  
340 *molitor*, *Drosophila* spp. (both adults and larvae), ants (*Lasius niger*), aphids (*Acyrtosiphon pisum*)  
341 and bean weevils (*Acanthoscelides obtectus*), (ii) robust, working with relatively low resolution  
342 video images (640 x 480 px), imperfect and variable lighting conditions and moderate levels of  
343 visual occlusion and background variation, and (iii) accurate, as tracked coordinates of *T. molitor*  
344 were found to closely match (<10% of the body length of the insect away from) coordinates  
345 determined by human users. Furthermore, the system is inexpensive as the software makes use of  
346 only open-source tools and does not require specialised apparatus for experimental set ups or  
347 recording. Finally, the inclusion of a graphical user interface (GUI) for video analysis and R  
348 package, Rubitrail, for statistical analysis, aim to maximise accessibility to the user and allow for  
349 tracking analysis 'straight out of the box'.

## 350   **References**

351

- 352   Bates, D., Maechler, M., Bolker, B., & Walker, S. (2013). lme4: Linear mixed-effects models using  
353       Eigen and S4. R package version, 1(4).
- 354   Benjamini, Y., & Hochberg, Y. (2000). On the adaptive control of the false discovery rate in  
355       multiple testing with independent statistics. *Journal of Educational and Behavioral*  
356       *Statistics*, 25(1), 60-83.
- 357   Beyan, C., & Fisher, R. B. (2013, September). Detection of abnormal fish trajectories using a  
358       clustering based hierarchical classifier. In British Machine Vision Conference (BMVC),  
359       Bristol, UK.
- 360   Branson, K., & Bender, J. (2012). CTRAX—the caltech multiple walking fly tracker.  
361       <http://ctrax.sourceforge.net/>
- 362   Calenge, C. (2011). Analysis of animal movements in R: the adehabitatLT Package. *R Foundation*  
363       *for Statistical Computing: Vienna, Austria*.
- 364   de Chaumont, F., Coura, R. D. S., Serreau, P., Cressant, A., Chabout, J., Granon, S., & Olivo-Marin,  
365       J. C. (2012). Computerized video analysis of social interactions in mice. *Nature methods*,  
366       9(4), 410-417.
- 367   Colomb, J., Reiter, L., Blaszkiewicz, J., Wessnitzer, J., and Brembs, B. (2012). Open Source  
368       Tracking and Analysis of Adult Drosophila Locomotion in Buridan’s Paradigm with and  
369       without Visual Targets. *PLoS ONE* 7, e42247.
- 370   Dankert, H., Wang, L., Hoopfer, E. D., Anderson, D. J., & Perona, P. (2009). Automated monitoring  
371       and analysis of social behavior in Drosophila. *Nature methods*, 6(4), 297-303.
- 372   Dingemanse, N. J., Both, C., Drent, P. J., Van Oers, K., & Van Noordwijk, A. J. (2002).  
373       Repeatability and heritability of exploratory behaviour in great tits from the wild. *Animal*  
374       *Behaviour*, 64(6), 929-938.
- 375   Domenici, P., Booth, D., Blagburn, J. M., & Bacon, J. P. (2008). Cockroaches keep predators  
376       guessing by using preferred escape trajectories. *Current Biology*, 18(22), 1792-1796.
- 377   Gomez-Marin, A., Partoune, N., Stephens, G. J., Louis, M., & Brembs, B. (2012). Automated  
378       tracking of animal posture and movement during exploration and sensory orientation  
379       behaviors. *PloS one*, 7(8), e41642.
- 380   Götz, K. G., & Biesinger, R. (1985). Centrophobism in *Drosophila melanogaster*. *Journal of*  
381       *Comparative Physiology A*, 156(3), 329-337.
- 382   Hen, I., Sakov, A., Kafkafi, N., Golani, I., Benjamini, Y. (2004). The dynamics of spatial behavior:



383       how can robust smoothing techniques help. *J Neurosci Methods*, 133, 161–72.

384   Lochmatter, T., Roduit, P., Cianci, C., Correll, N., Jacot, J., & Martinoli, A. (2008, September).

385       Swistrack-a flexible open source tracking software for multi-agent systems. In *Intelligent*

386       *Robots and Systems*, 2008. IROS 2008. IEEE/RSJ International Conference on (pp. 4004-

387       4010). IEEE.

388   Martin, J.R. (2004). A portrait of locomotor behaviour in *Drosophila* determined by a video-

389       tracking paradigm. *Behav. Processes* 67, 207–219.

390   Noldus, L. P., Spink, A. J., & Tegelenbosch, R. A. (2001). EthoVision: a versatile video tracking

391       system for automation of behavioral experiments. *Behavior Research Methods, Instruments,*

392       & *Computers*, 33(3), 398-414.

393   Robie, A.A., Straw, A.D. & Dickinson, M.H. (2010) Object preference by walking fruit flies,

394       *Drosophila melanogaster*, is mediated by vision and graviperception. *The Journal of*

395       *Experimental Biology* 213: 2494–506.

396   Straw, A. D., & Dickinson, M. H. (2009). Source Code for Biology and Medicine. Source code for

397       biology and medicine, 4, 5.

398   Swierczek, N. A., Giles, A. C., Rankin, C. H., & Kerr, R. A. (2011). High-throughput behavioral

399       analysis in *C. elegans*. *Nature methods*, 8(7), 592-598.

400   Valente, D., Golani, I., & Mitra, P.P. (2007) Analysis of the trajectory of *Drosophila melanogaster* in

401       a circular open field arena. *PloS one* 2: e1083.

402   Venables, W. N., & Ripley, B. D. (2010). Package ‘MASS’. Online at: [http://cran.r-project.](http://cran.r-project.org/web/packages/MASS/MASS.pdf)

403       [org/web/packages/MASS/MASS.pdf](http://cran.r-project.org/web/packages/MASS/MASS.pdf).

404   Yaski, O., Portugali, J., & Eilam, D. (2011). Arena geometry and path shape: When rats travel in

405       straight or in circuitous paths?. *Behavioural brain research*, 225(2), 449-454.



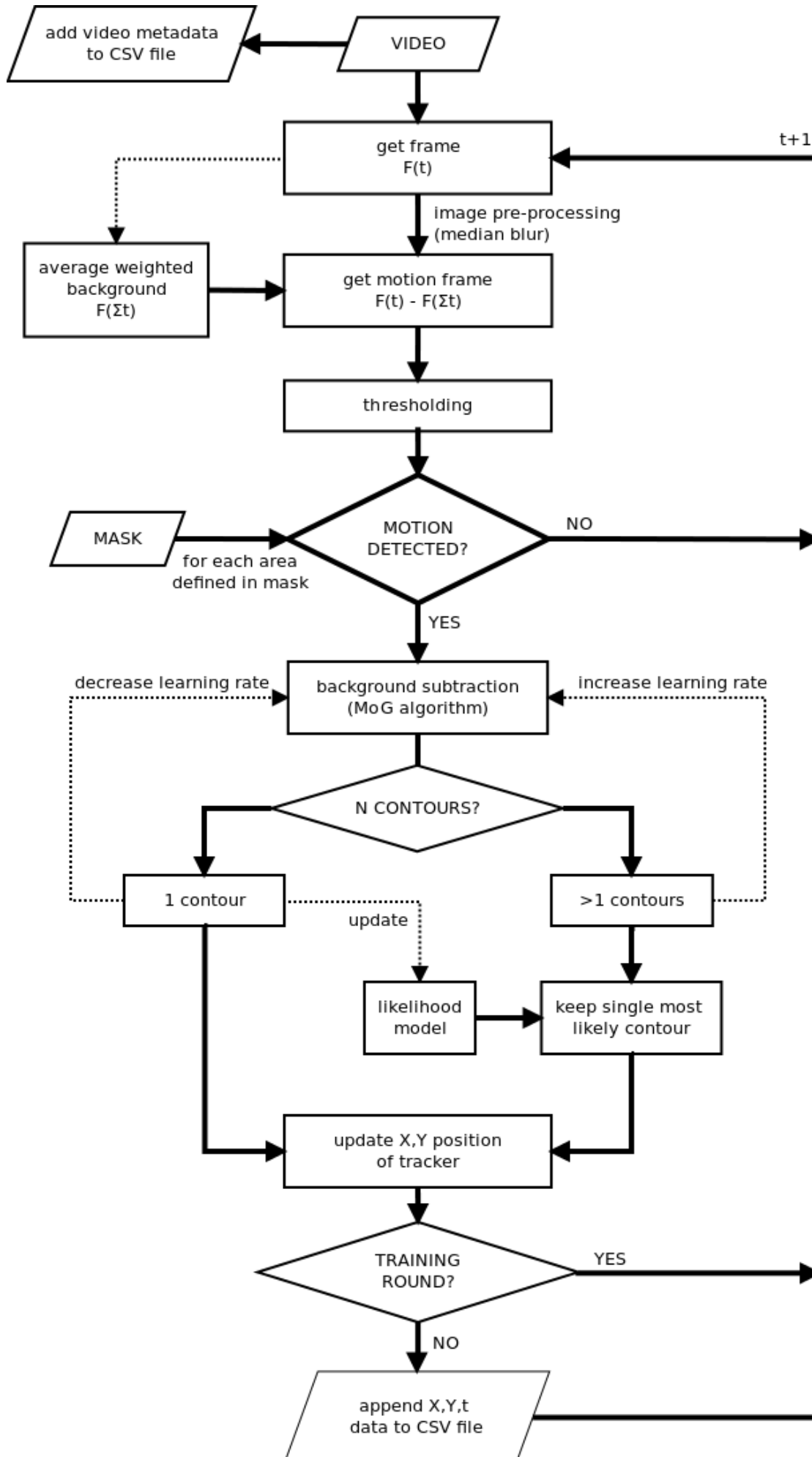


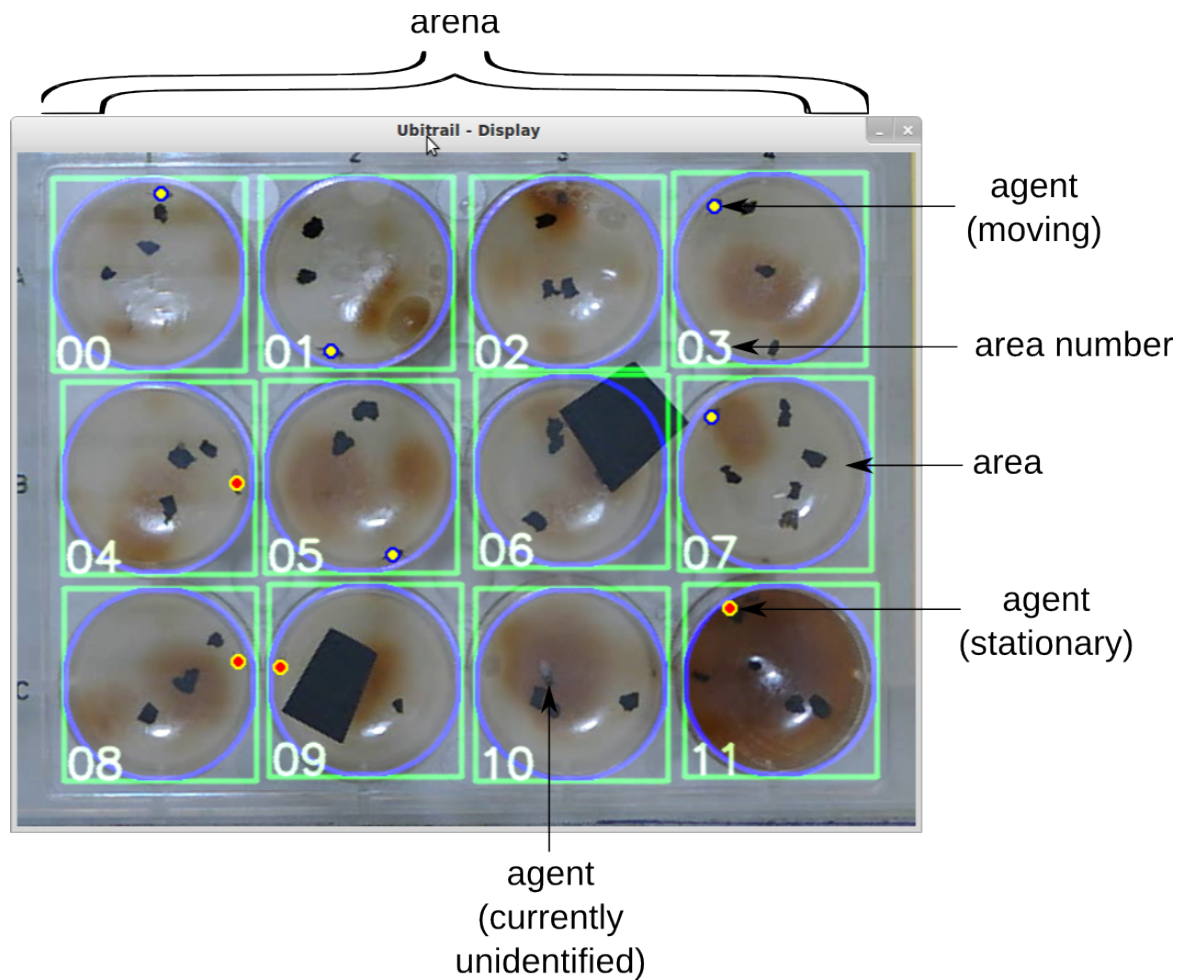
**Figure 1.** Flow diagram of tracking software process. Ubitrail takes a digital video file as input and returns a CSV file containing tracked X,Y-coordinates for each frame in each defined area, as well as a header containing metainformation extracted from the video. Each frame,  $F(t)$ , is extracted individually from the video and de-noised using a (9x9) median blur filter. A motion frame is then produced by subtracting the current frame from a running weighted average of previous frames,  $F(t-1)$ , which is used to model the background. At this point, the mask is applied to split the frame up into individual areas. In areas where motion is detected, a dynamic learning algorithm based upon a mixture of Gaussian (MoG) background subtraction method is used to identify moving foreground objects. The MoG algorithm is trained separately for each individual area, with the rate of learning being increased following ambiguous frames in which the movement of more than one foreground object is detected, and decreased following unambiguous in which movement of exactly one foreground object is detected. In order to solve ambiguities in foreground detection, an on-the-fly likelihood model is built based upon several key features of known foreground objects, including contour shape, mean and standard deviation of pixel colour in the red, green and blue channels, and distance between centre of the current contour and centre of the last detected contour. A log-likelihood,  $L$ , is then calculated under the assumption of normal distribution, where:

$$L = \sum_{i=0}^n l_i$$

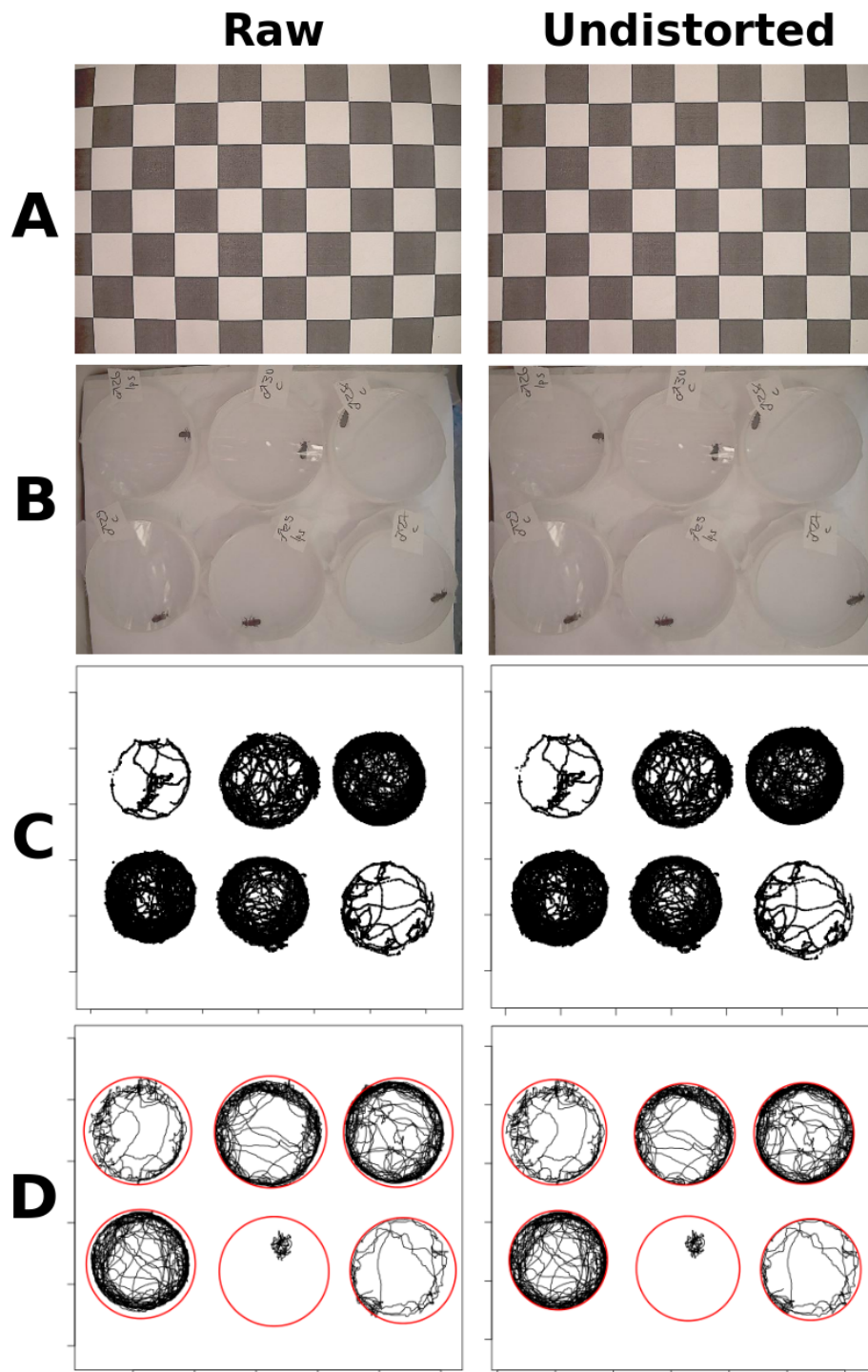
$$l_i = \ln \left( \frac{1}{s_i \sqrt{2\pi}} e^{-\frac{(x_i - m_i)^2}{2s_i^2}} \right)$$

and where  $n$  is the total number of features,  $i$  is a given feature,  $x_i$  = value of feature  $i$ ,  $m_i$  is the psuedo-mean of feature  $i$ , and  $s_i$  is the pseudo-standard-deviation of feature  $i$ . When more than one contour is detected, the contour with the maximum log-likelihood is taken as the foreground object. An initial training round (default = 500 frames) is used to train the background subtraction

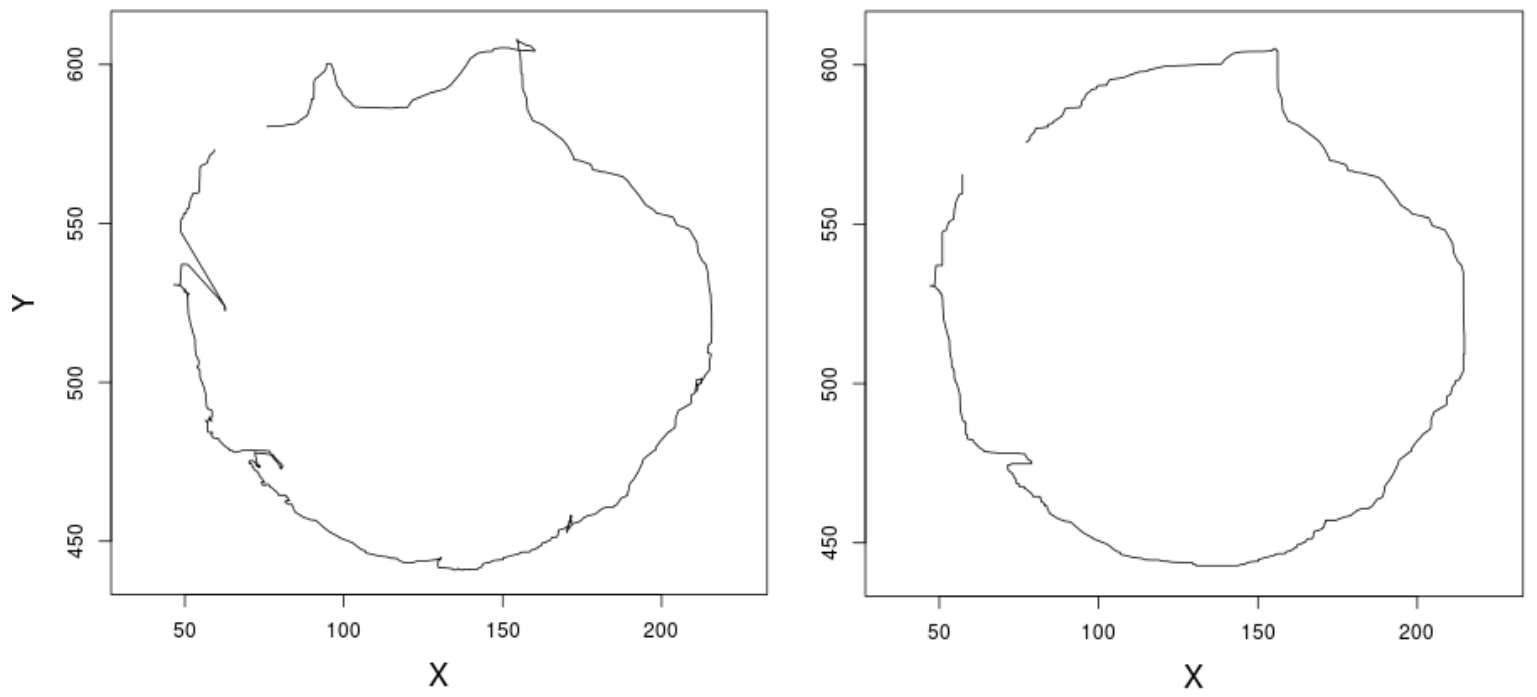
433 algorithm and build a suitable likelihood model for foreground detection, ensuring valid foreground  
434 detection throughout the video analysis.



436 **Figure 2.** The graphical user interface (GUI) of the Ubitrail software, with key elements labelled.  
 437 The outline of the mask which defines each individual arena is shown in blue, with its assigned area  
 438 number depicted inside the green square. The above sample shows a test on *Drosophila*  
 439 *melanogaster* adults, where variation in background luminosity was created to test for the  
 440 robustness of background subtraction, and covering objects (unlabelled black objects) were  
 441 introduced to test for the effects of occlusion upon insect tracking.

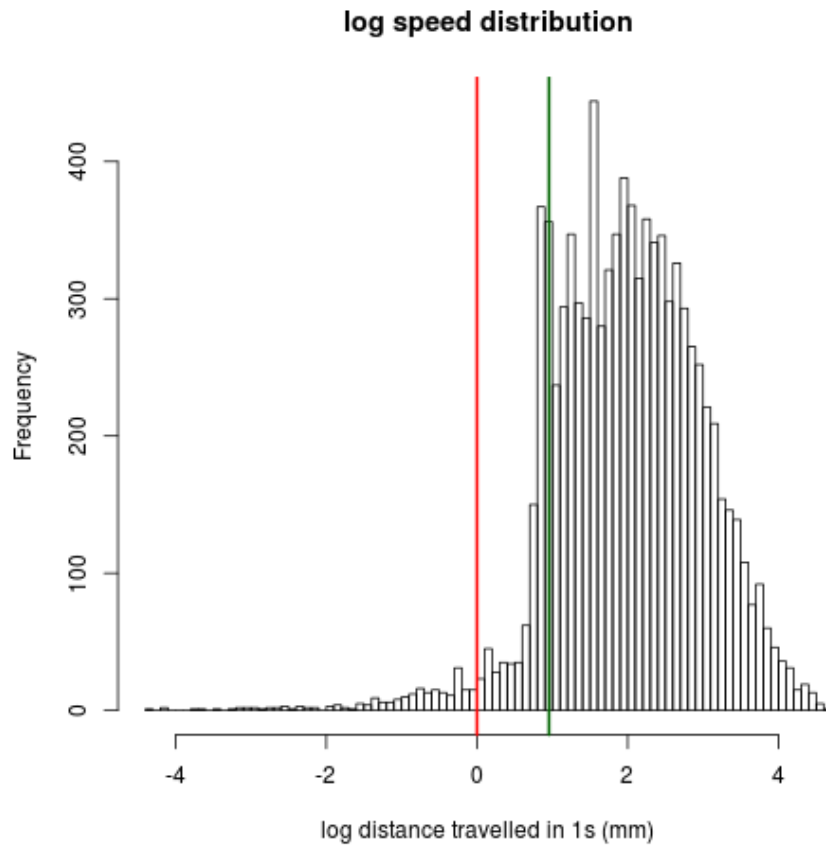


442 **Figure 3.** The effects of lens undistortion upon images and tracked coordinates. (A) An image of a  
443 chessboard pattern is captured during the recording stage and used to calibrate parameters for an  
444 undistortion matrix. The effects of undistortion (raw [left] vs. processed [right]) are shown for (B)  
445 raw video frames, (C) tracked movement vectors, and (D) fitting a minimal enclosing circle to  
446 arenas.

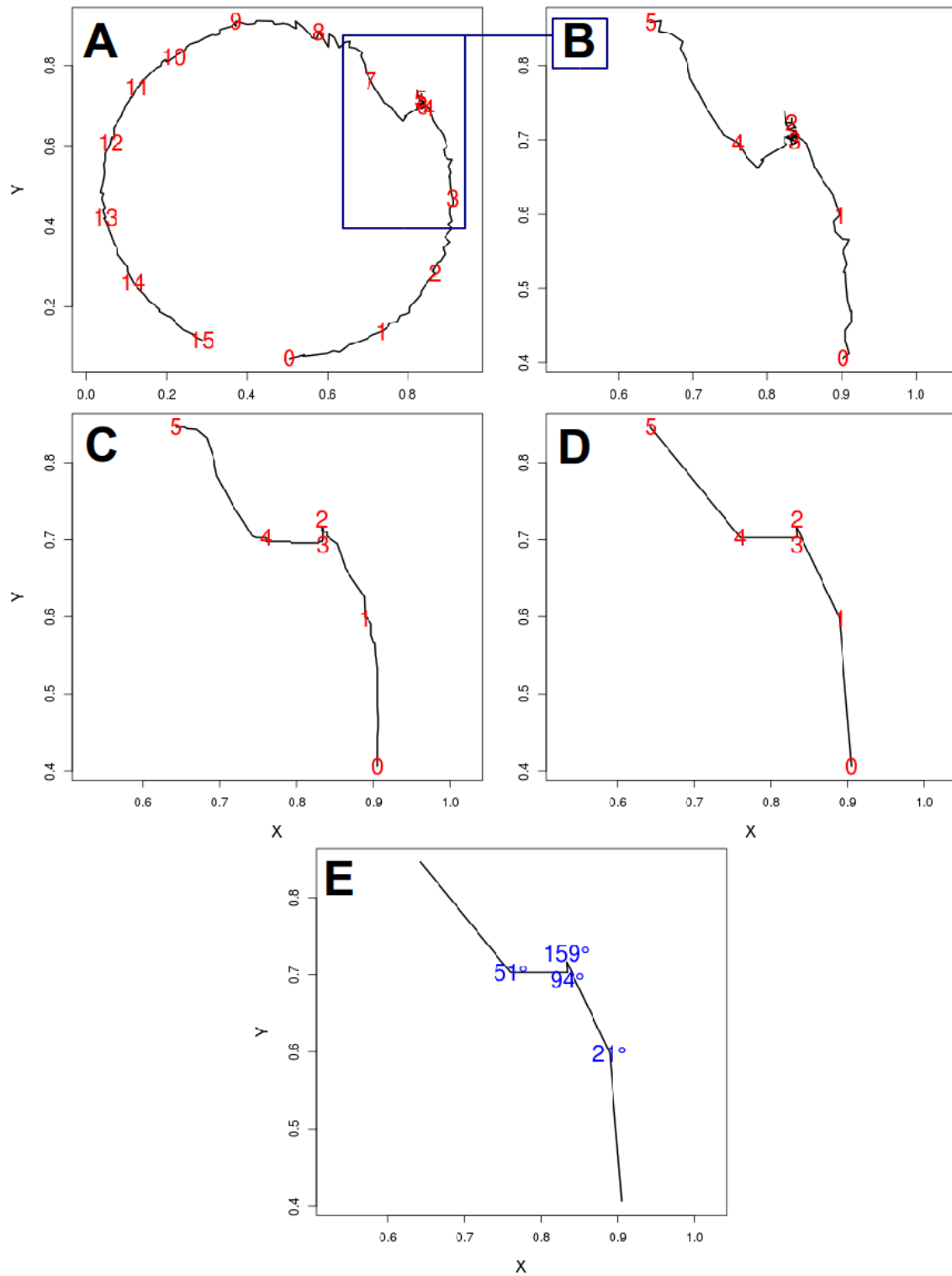


447 **Figure 4.** Smoothing of tracked x,y-coordinates. (A) shows a 60s sample of raw trajectories  
 448 outputted by the tracking software, whilst (B) shows the same trajectory after application of a  
 449 rolling median with window size of 3s (60 frames).



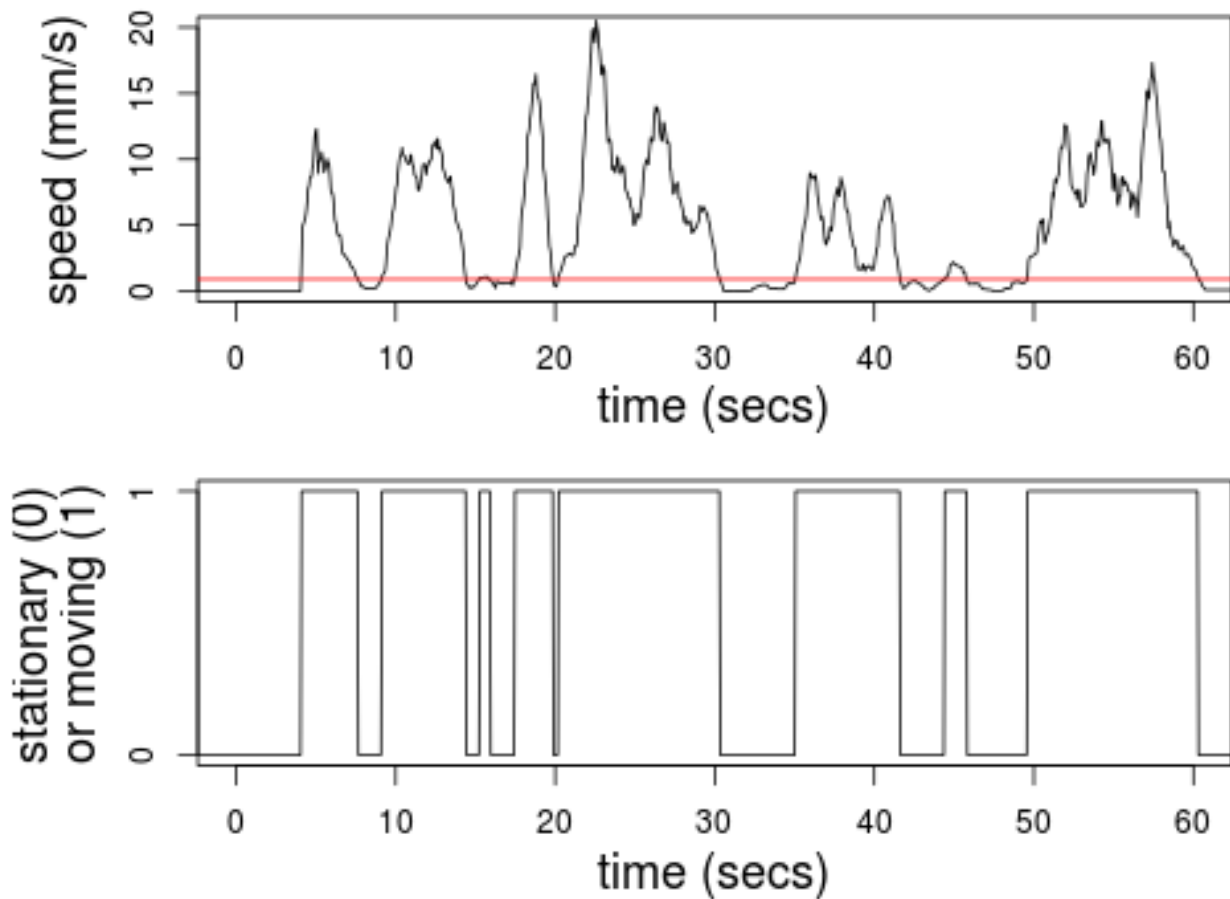


450 **Figure 5.** Histogram of smoothed velocity frequency (logarithmic scale), with lower threshold (red  
451 line: 0 mm/s) and upper thresholds defined (green line: 1 mm/s)

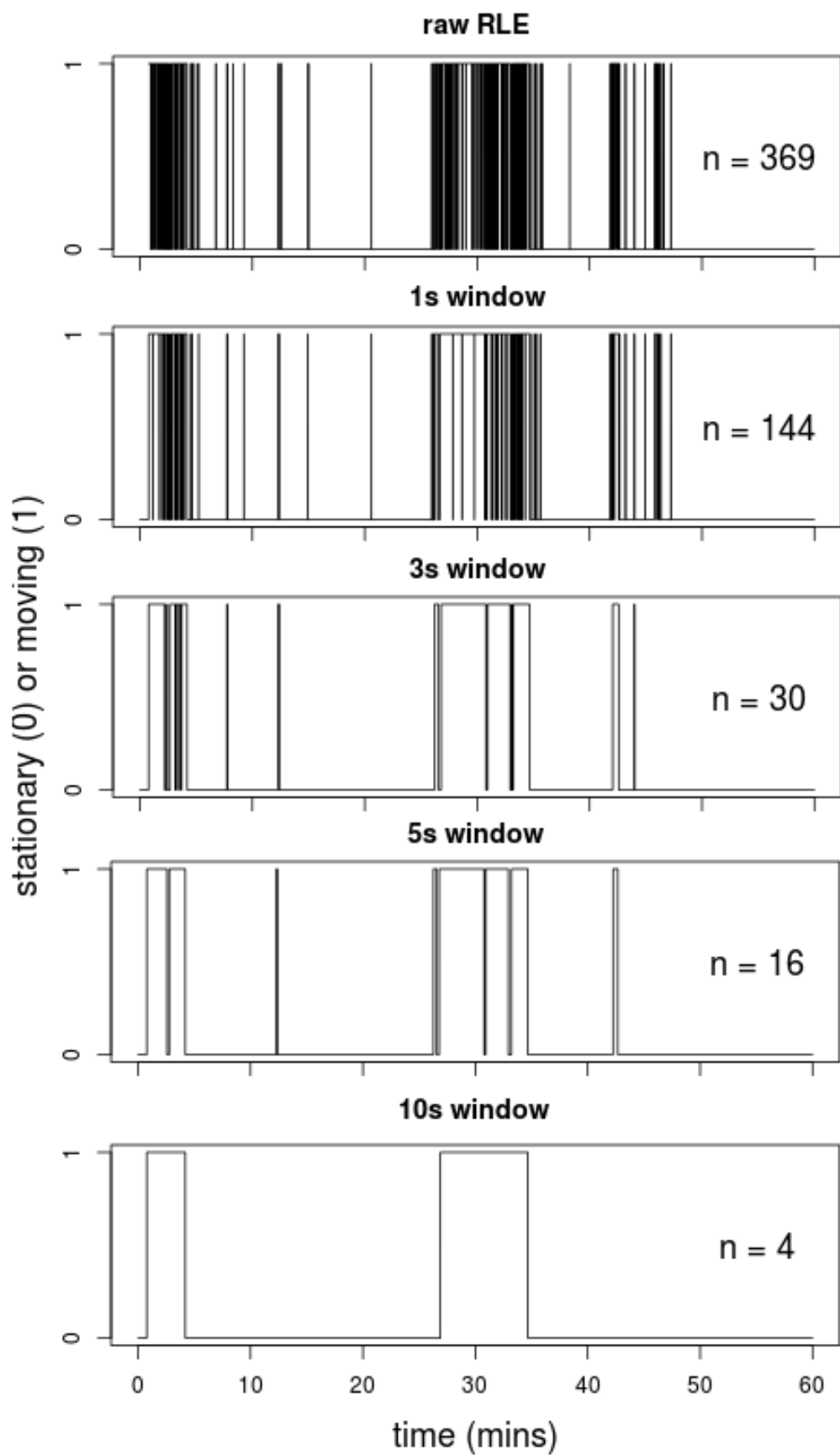


452 **Figure 6.** Calculation of turning angles. (A) shows a 15s sample (300 frames) of raw tracked X,Y-  
 453 coordinates, with corresponding number of seconds overlaid (red text). The area inside the blue box  
 454 is a 5s subsample which is zoomed on in (B-E), where (B) shows the same raw X,Y-coordinates  
 455 with number of seconds (red text), (C) shows coordinates that have been smoothed using a rolling  
 456 median with a window of 20 frames [1s]), (D) shows coordinates that have been smoothed

457 (window=20) and then resampled at 20Hz (1 frame per s), and (E) shows the final relative turning  
458 angles (in degrees; blue text) calculated from smoothed and resampled coordinates in (D).

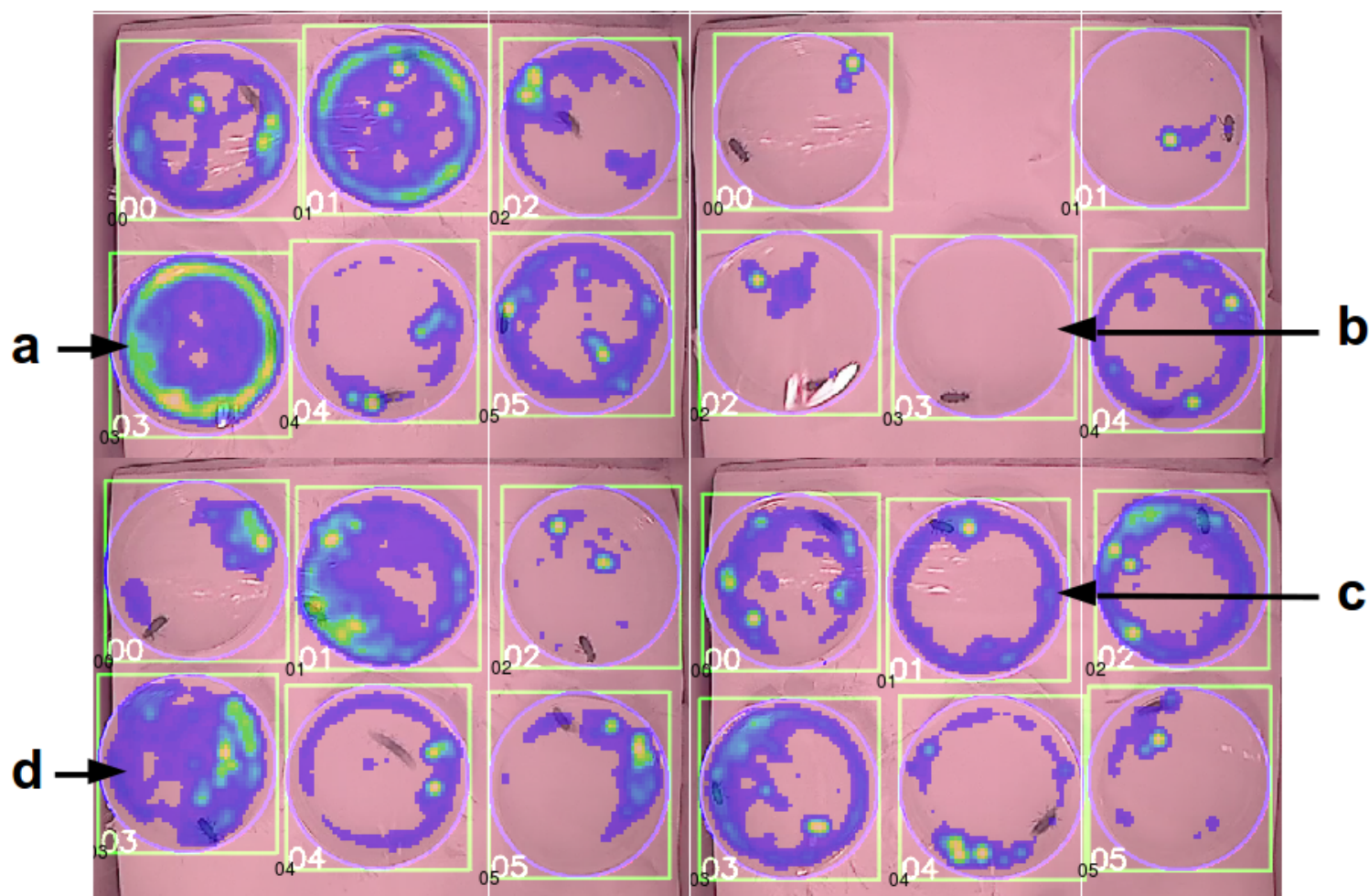


460 **Figure 7.** Determination of insect movement (mobile vs. stationary) using run length encoding. (A)  
 461 shows a 60s sample of smoothed insect movement speed (mm/s). The red line represents the user-  
 462 defined speed threshold (here, 1mm/s) below which the insect is classified as being stationary. (B)  
 463 shows the same sample with speed run length encoded into a binary format, whereby the insect is  
 464 classified as mobile (1) when moving faster than the speed threshold and stationary (0) when  
 465 moving slower.

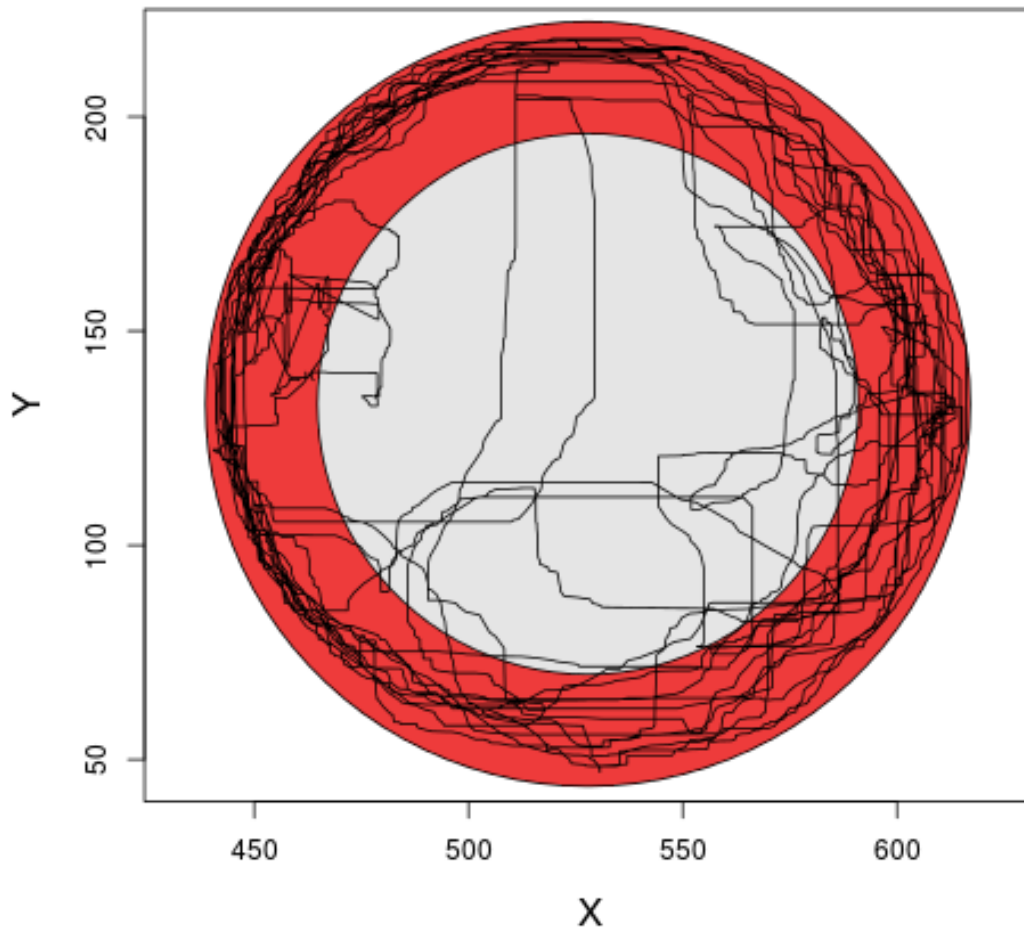


467 **Figure 8.** A sample of different sliding window sizes for smoothing run length encoded movement  
 468 data, from raw data (1 frame interval) to 10s (200 frame interval). n indicates the number of defined

469 transitions between mobile and stationary phases, which can be seen become eroded as the size of  
470 the sliding window increases. A sliding window of 3s was used in the final analysis as this was  
471 found to preserve biologically meaningful pausing events whilst still reducing noise from  
472 oversampling.

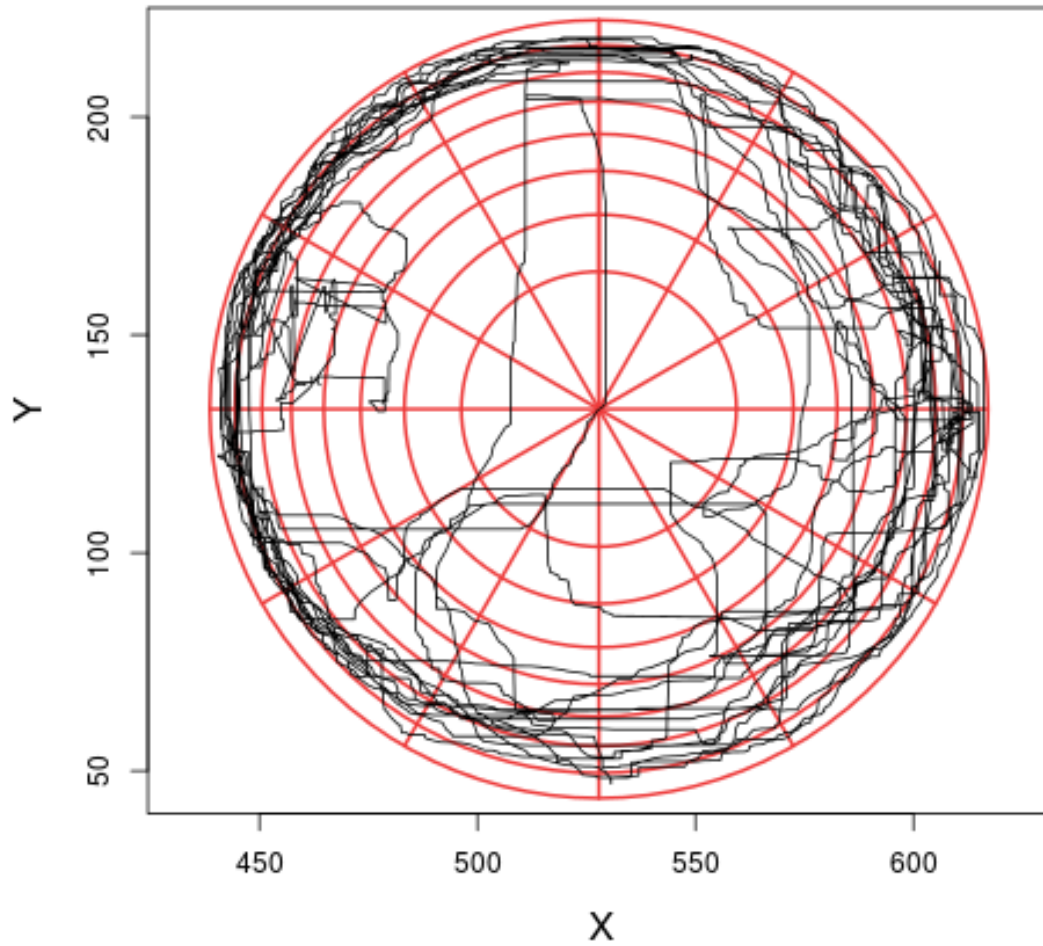


474 **Figure 9.** Sample 'heatmaps' showing the frequency insect locations over the course of a 60 minute  
 475 recording, with yellow areas being visited frequently and blue areas infrequently. Each background  
 476 image is a frame taken from the raw video analysed by the tracker. (a) shows an insect which  
 477 displayed a high level of exploration as well as a relatively high degree of thigmotaxis. (b) shows an  
 478 insect which did not display sufficient movement during the recording to be tracked (<500 frames  
 479 [25s] in which motion was detected). (c) shows an insect with a high degree of thigmotaxis but a  
 480 relatively low level of exploration. (d) shows an insect with a high level of exploration, although  
 481 with movement being concentrated primarily on the right hand side of the arena.



482 **Figure 10.** Visualisation of the thigmotaxis metric. A minimum enclosing circle (outer boundary of  
 483 red ring) is fitted to each circular arena, which is then divided into two zones of equal area, an inner  
 484 zone (shown in red) and an outer zone (shown in grey). The radius of the inner circle,  $r_{inner}$ , is  $\sqrt{2}$   
 485 times smaller than the radius of the outer enclosing circle,  $r_{outer}$ . Each X,Y-coordinate in a trajectory  
 486 path (black line) is  $\sqrt{(x_{mid} - x_t)^2 + (y_{mid} - y_t)^2} > \frac{r_{outer}}{\sqrt{2}}$   
 487 designated as being in  
 488 the inner or outer zone based upon its Pythagorean distance from the midpoint of the arena. I.e. a  
 489 coordinate  $(x_t, y_t)$  is classified as being in the outer zone if:





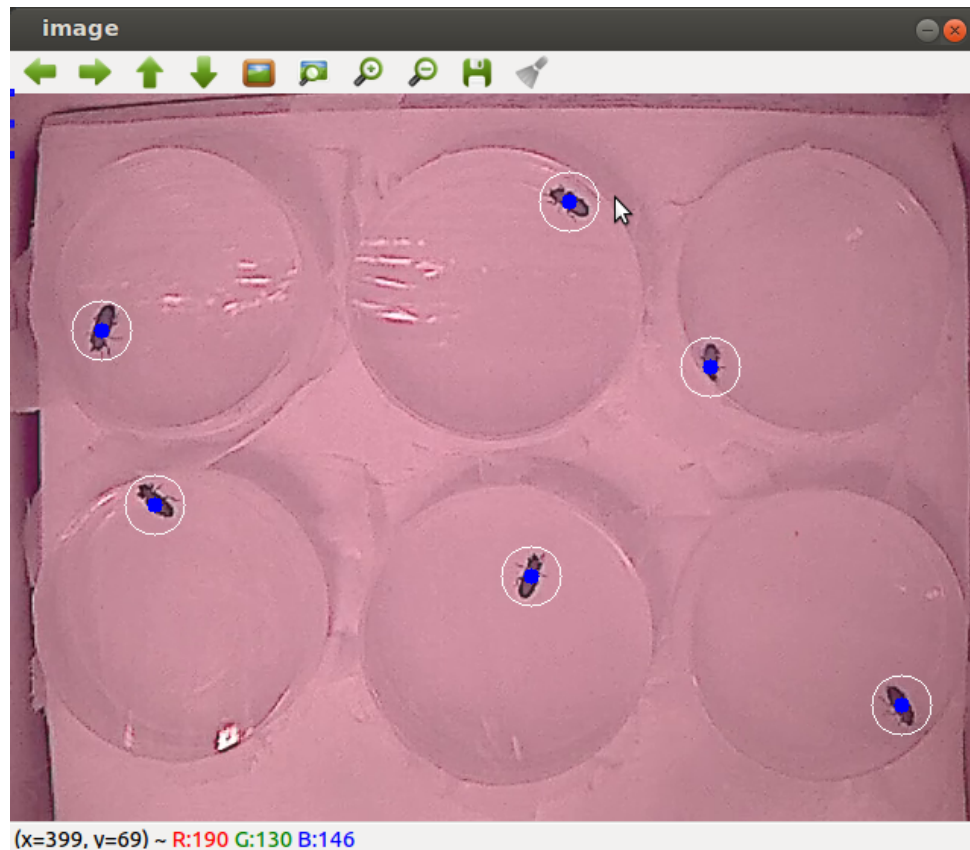
490 **Figure 11.** Visualisation of the exploration metric. A minimum enclosing circle is fitted to each  
 491 circular arena, which is then divided into a network of grid cells of equal area by concentric circles  
 492 and line segments. Here, 8 concentric circles and 12 line segments (shown above in red) compose a  
 493 grid of 96 cells. Given a number of circles  $i:n$ , the radius of circle  $i$ ,  $r_i$ , is given by the formula:

$$r_i = r_n \cdot \sqrt{\frac{i}{n}}$$

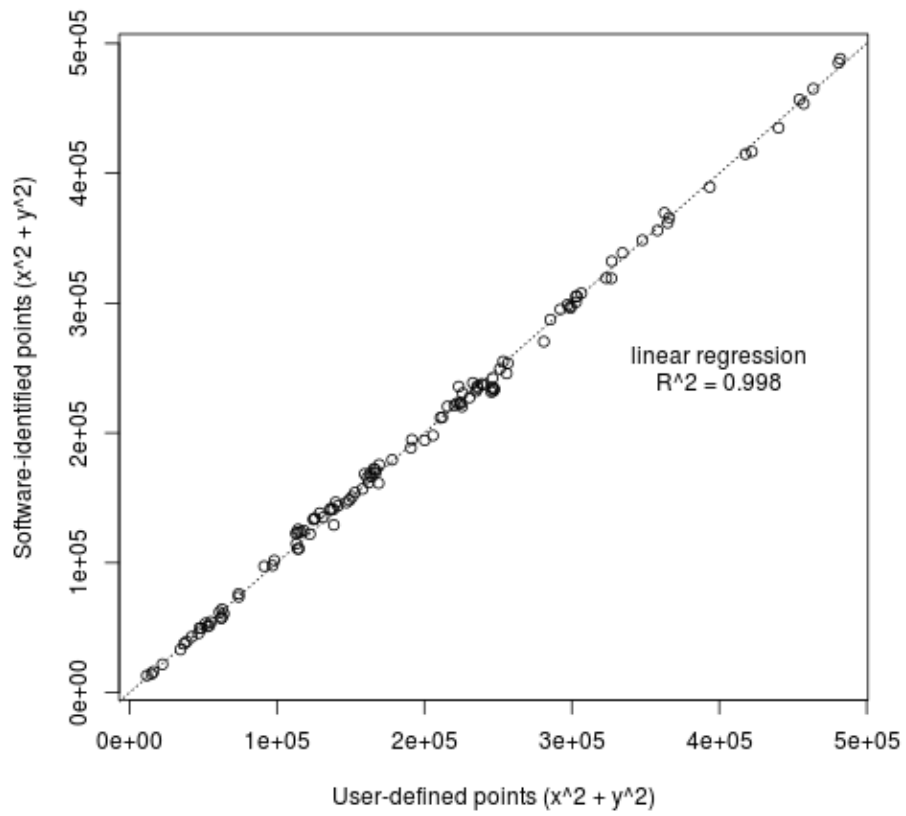
495 where  $r_n$  is the radius of the outermost circle enclosing the arena. Given a number of line segments,  
 496  $j:n$ , the angle of segment  $j$ ,  $\theta_j$ , is given by the formula:

$$\theta_j = \frac{2\pi j}{n}$$

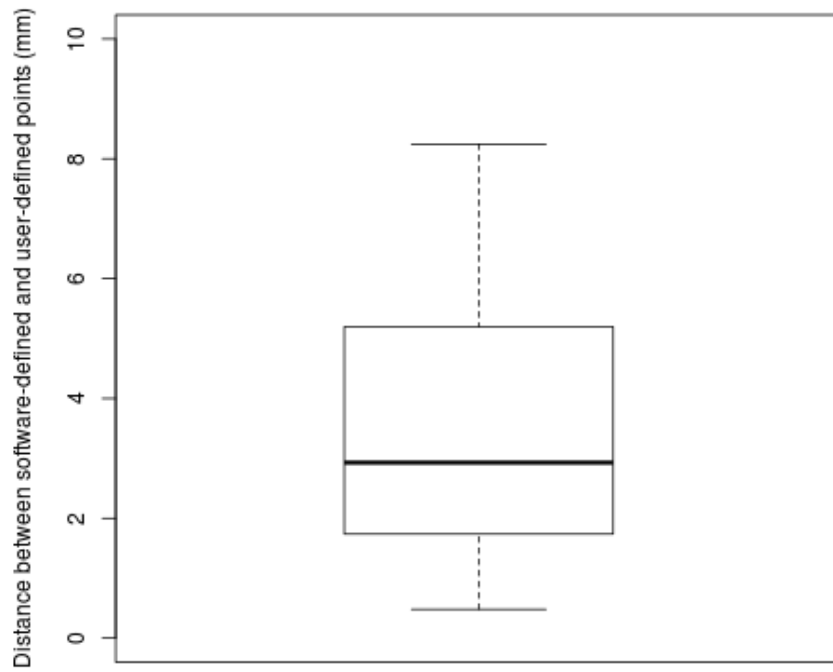
498 The cell location of each coordinate in a smoothed trajectory path (shown above in black) is then  
499 determined, and the total number of unique cells visited by the insect used as a measure of  
500 exploration.



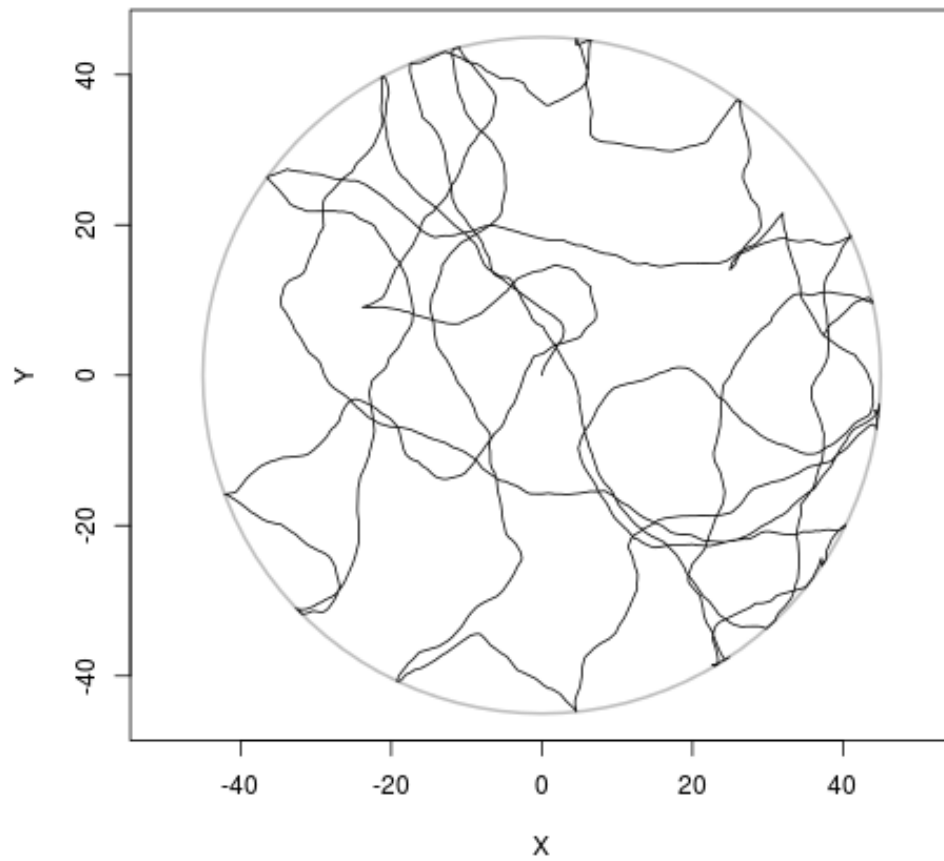
502 **Figure 13.** A sample of the human scoring test application used to examine automated tracking  
 503 accuracy. Raw frames were randomly extracted from a video and opened in a simple C++  
 504 application. Users then clicked the point at which they deemed the centre of mass of insect to be  
 505 (shown as blue dots with white circle). User-defined x,y-coordinates were then compared with  
 506 coordinates defined by the tracking software for the same frames (see Figures 14 & 15).



507 **Figure 14.** Correlation between user-defined X,Y-coordinates of insect location (groundtruth data)  
 508 and X-Y-coordinates outputted by the automated tracker for the same frames.

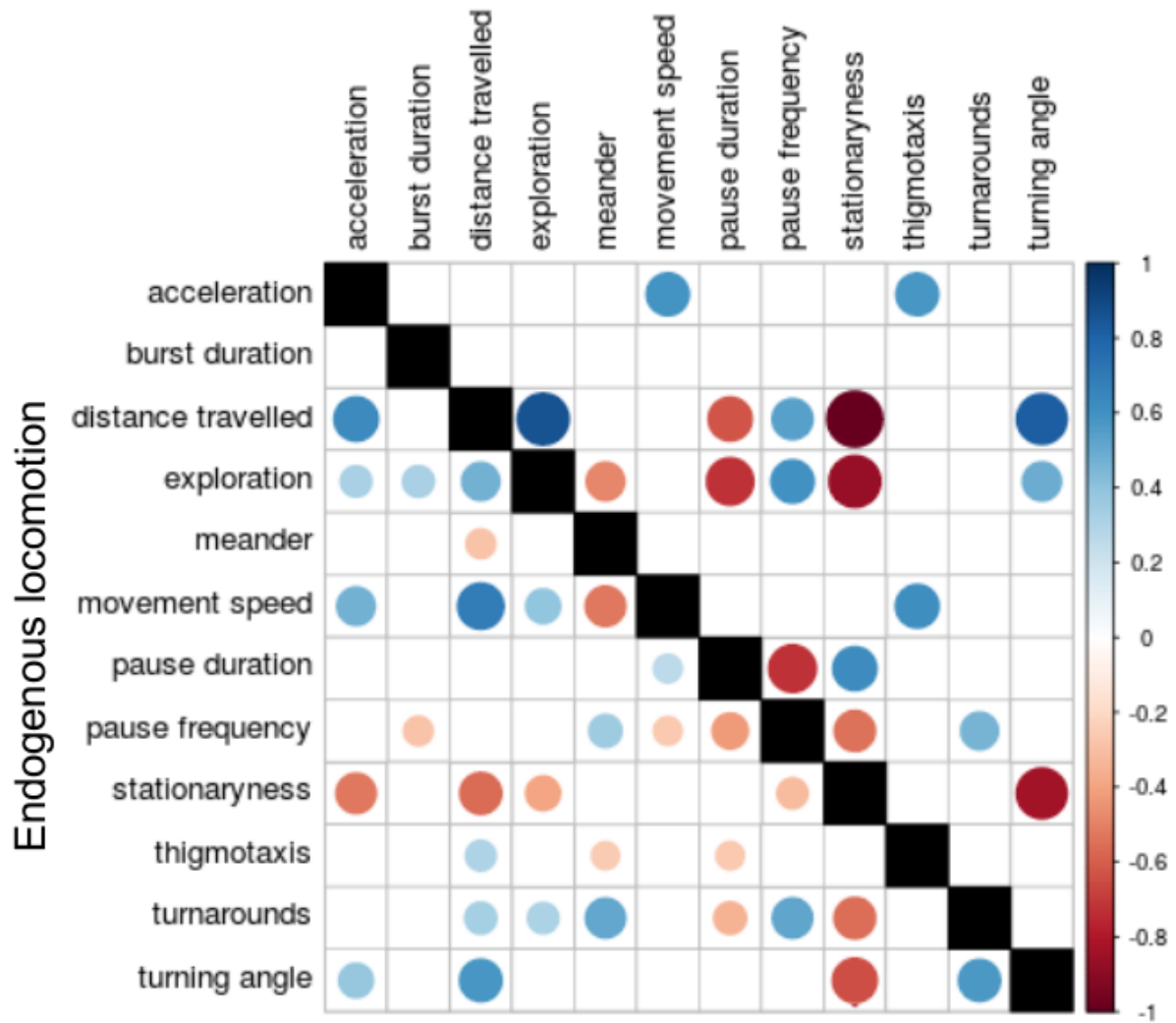


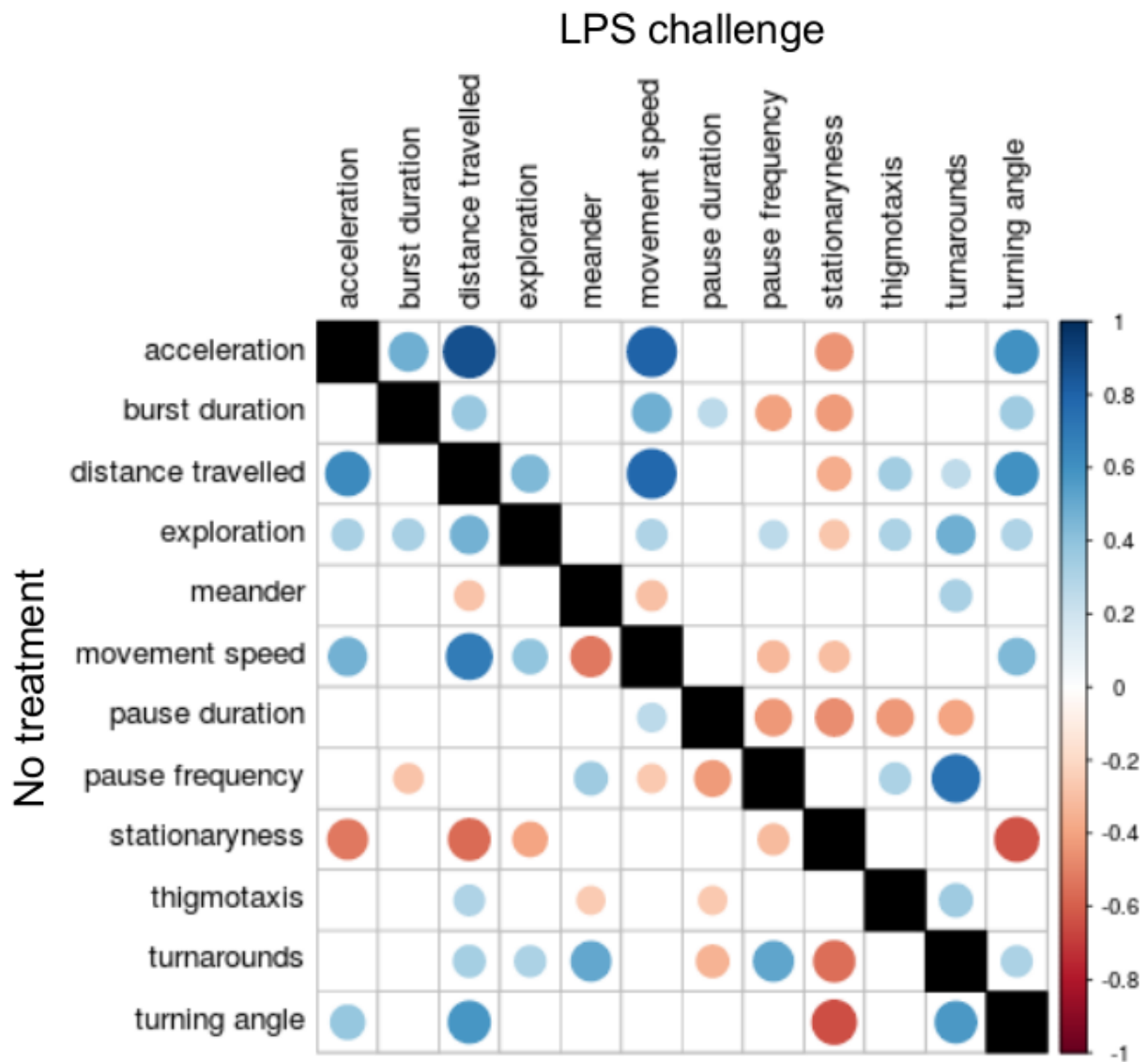
510 **Figure 15.** Boxplot showing Pythagorean distance (in mm) between tracked X,Y-coordinates of  
511 insects outputted by the software and coordinates defined by users. Boxplots show the median and  
512 interquartile range (IQR), and whiskers represent  $1.5 \times \text{IQR}$ . For comparison, the mean body length  
513 of an adult *T. molitor* is 18mm.



514 **Figure 16.** Sample trajectory of a correlated walk simulation lasting 10 minutes at 20 frames per  
515 second. The outer bounds of the simulated arena are defined by the grey circle.

## Simulated locomotion

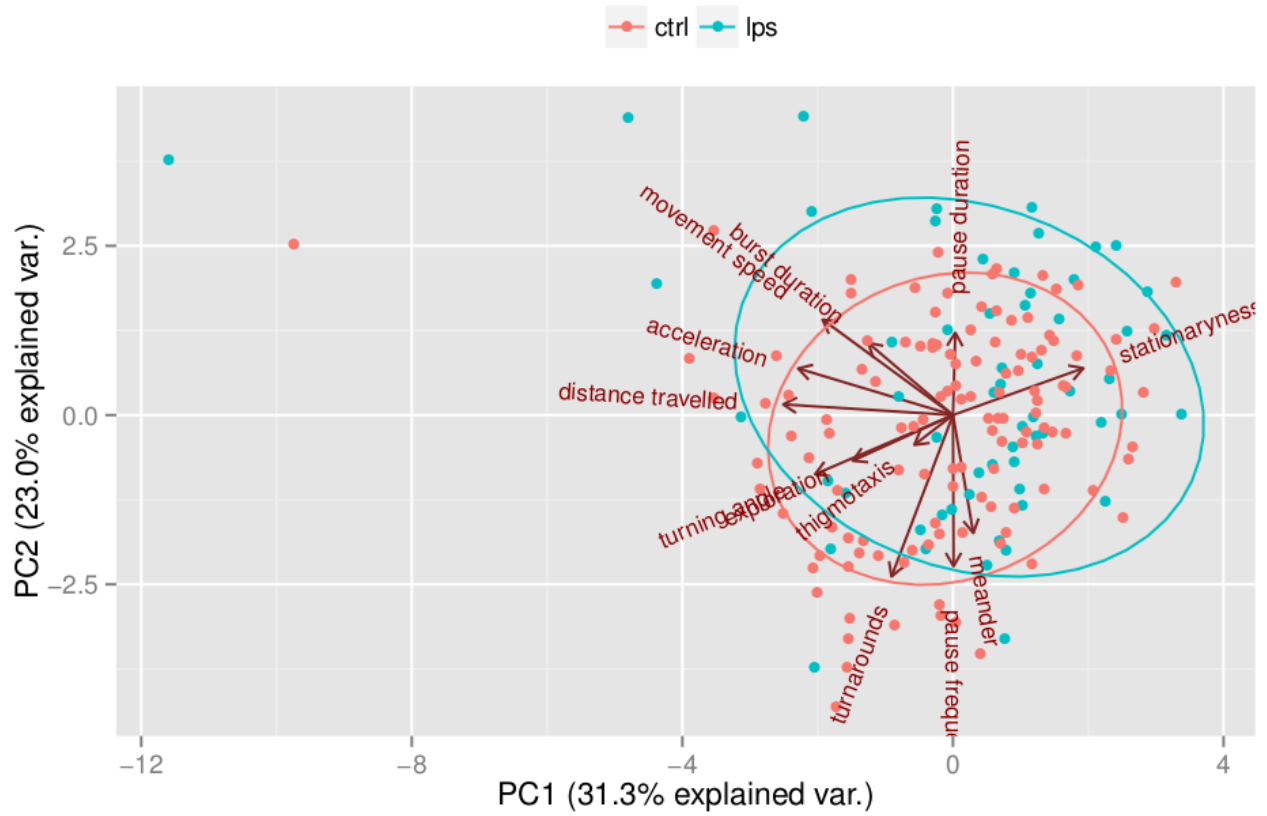




518 **Figure 17.** Correlation plots showing the relationships between defined behavioural metrics. The  
 519 order of the variables was set by clustering them for endogenous locomotion data (A, lower left  
 520 part). Only significant correlations ( $p < 0.05$ ) are shown, with larger circles representing greater  
 521 significance. Each matrix is divided into two triangles representing the correlations between the  
 522 same behavioural metrics extracted from different datasets. (A) Correlation matrices comparing  
 523 endogenous beetle locomotion with simulated correlated walks, showing correlations in untreated  
 524 beetles (lower left triangle) and correlated walk simulations (upper right triangle). (B) Correlation  
 525 matrices comparing the effects of an immune challenge upon endogenous beetle locomotion,



526 showing correlations in unchallenged beetles (lower left triangle) and beetles challenged with LPS  
527 (upper right triangle).



529

530 **Figure 18.** Principle component analysis (PCA) showing the effect of immune challenge upon

531 locomotory behaviour in *T. molitor*.

532 <TODO: Figure of sample results from *T. molitor*>

533

534 **Figure 19.** The effect of immune challenge (unchallenged in blue, LPS challenged in red) on

535 behavioural metrics in *T. molitor* males and females. Bars show means ( $\pm$  S.E.) of single values for

536 C,F,I,J,K. and means ( $\pm$  S.E.) of medians for A,B,D,E,G,H.